Research Square

Preprints are preliminary reports that have not undergone peer review.
They should not be considered conclusive, used to inform clinical practice,
or referenced by the media as validated information.

Evaluating Future Warming Scenarios in mainland India based on Bias-Corrected CMIP6 Multi-Model Ensembles

Avijit Paul

engr.avijit.paul@gmail.com

Central Institute of Technology Kokrajhar Deemed to be University https://orcid.org/0000-0001-9388-9571

Monomoy Goswami

Central Institute of Technology Kokrajhar Deemed to be University

Research Article

Keywords: Future temperature projections of India, Future Temperature trends of India, CMIP6, Bias Correction, Multi Model Ensemble

Posted Date: April 6th, 2026

DOI: https://doi.org/10.21203/rs.3.rs-9241553/v1

License: This work is licensed under a Creative Commons Attribution 4.0 International License.
Read Full License

Evaluating Future Warming Scenarios in mainland India based on Bias-Corrected CMIP6 Multi-Model Ensembles

Avijit Paul* and Monomoy Goswami
Department of Civil Engineering, Central Institute of Technology Kokrajhar, Kokrajhar, India
Email: engr.avijit.paul@gmail.com; monomoy99@hotmail.com
*Corresponding author

Abstract

Understanding the spatio-temporal variability of temperature and its future evolution is critical for climate impact assessment and adaptation planning over India, a region characterized by complex physiography and pronounced climatic heterogeneity. This study presents a comprehensive assessment of future variations in monthly maximum, minimum, and mean temperatures over mainland India using outputs from Coupled Model Intercomparison Project Phase 6 (CMIP6) global climate models. To address climate model deficiencies, raw model outputs are bias-corrected and combined using an optimized multi-model ensemble framework. The resulting ensemble is applied to generate high-resolution temperature projections for the period 2025–2100 under four Shared Socioeconomic Pathway scenarios (SSP1-2.6, SSP2-4.5, SSP3-7.0, and SSP5-8.5) to identify the most vulnerable regions for future warming. Spatio-temporal analyses reveal a consistent warming signal across the country, with the magnitude and spatial coverage of warming increasing markedly under higher-emission pathways. Regions characterized by complex topography, particularly the Himalayan and north-eastern areas, exhibit enhanced warming relative to the national average. Across all scenarios, monthly minimum temperature is projected to increase more rapidly than monthly maximum temperature, indicating intensified nocturnal warming and a progressive reduction in the monthly temperature range. These findings provide robust scientific evidence for anticipated temperature changes over India and offer valuable insights for climate risk assessment, policy formulation, and sustainable planning in climate-sensitive sectors.

Keywords: Future temperature projections of India, Future Temperature trends of India, CMIP6, Bias Correction, Multi Model Ensemble

1. Introduction

Temperature is a fundamental climate variable that governs the environment, agriculture, water resources, energy demand etc. (Frederick and Major, 1997) of any geographical region, and serves as an indicator of the past, present and future state of climate thereof. Spatially, different regions of the vast expanse of the landmass of India are characterized by diversities in physiographic and climatic features, making these especially sensitive to changes in temperature resulting from global climate change. The impacts of the changes in temperature, manifest in many ways. Amongst these are the increases in frequency and magnitude of the occurrence of extreme weather-related events, such as heatwaves, wildfires, excessive rainfall causing pluvial and fluvial floods, severe storms, deficient rainfall causing droughts, etc., besides the impacts on cellular, organismal and macroecological functions across all scales of life, physiological stress and bodily damage to humans, livestock, poultry, fish, and agricultural crops (Asseng et al., 2021), etc. Having information on the likely values of the temperature over different regions of the country and the country as a whole in the future is therefore highly important for strategic planning for sustainable development, preparing for climate change (Revadekar et al., 2012), ensuring ecosystem balance and fuelling economic growth. Among the most critical indicators of these changes are the average monthly and annual values and the trends particularly related to

(i) monthly maximum temperature (T_{max}) that directly govern the intensity of heatwaves (Perkins-Kirkpatrick and Gibson, 2017), heat stress on humans (Huang et al., 2024), livestock (Thornton et al., 2021), wildlife (Stillman, 2019), and phenological shifts besides influencing evaporation rates (Linacre, 1977), agricultural and domestic water demand (Li et al., 2020), wildfire risk (Peng et al., 2023), and peak energy loads for cooling (Wan et al., 2011);

(ii) monthly minimum temperature (T_{min}) that affect crop development (Atkinson and Porter, 1996), pest and disease cycles (Sutherst et al., 2011), frost occurrence which can be either beneficial or detrimental depending on crop and season (Sakai and Larcher, 1987), and phenological shifts; and

(iii) monthly mean temperature (T_{mean}) that influence long-term biological processes (Burgmer and Hillebrand, 2011), energy demand for heating/cooling over seasons (Shen

and Liu, 2016), phenological shifts, etc. and serve as fundamental inputs for many climate impact models.

The objective of this current study was set to estimate the future values of the three temperature variables and the changes of the key statistics of these variables relative to the corresponding historical values, and to explore the trends of variations of these variables over mainland India considering different future projections and identify the most vulnerable regions. The projections were considered for four scenarios (SSP1-2.6, SSP2-4.5, SSP3-7.0 and SSP5-8.5) of likely climate change impacts of the future along Shared Socioeconomic Pathways (SSPs) that include population growth, economic development, energy use, and policy choices (Riahi et al., 2017) as determinants of Green-House Gas (GHG) emissions, and hence climate change impacts from GHG concentrations.

2. Study Area and Datasets

2.1 Study Area

In this study, mainland India excluding the islands, covering an area of 3.287 million km² lying between latitudes 6°N and 36°N and longitudes 68°E and 98°E approximately, was considered. Geographically, India is the seventh-largest country in the world, and is bounded by the Himalayas on the north that extends on the northeast, the Bay of Bengal and the Arabian Sea forming the eastern and the western coastlines, and the Indian Ocean on the south. The vast expanse of this study area is divided into seven temperate regions by the Indian Institute of Tropical Meteorology (IITM), Pune according to spatial and temporal variability of surface air temperature (Dash and Mamgain, 2011). These regions are: Western Himalaya (WH), North Central (NC), North West (NW), North East (NE), Indian Peninsula (IP), East Coast (EC) and West Coast (WC), and are presented in Figure 1(a). The occurrence of these temperate regions reflects the atmospheric conditions under broader climatic systems that differently influence different parts of the country. Based on the widely-used Köppen–Geiger system of classification of climate, India is divided into seven climatic regions, each having one of the seven climate types named Tropical Monsoon (Am), Tropical Savannah (Aw), Arid Desert Hot (Bwh), Arid Steppe Hot (Bsh), Arid Desert Cold (Bwk), Temperate Dry Winter Hot Summer (Cwa) and Temperate Dry Winter Warm Summer (Cwb). These divisions are shown in Figure 1(b) (Upadhyaya and Ramsankaran, 2017), and are characterized by distinct ranges of daily

temperature and distinct temporal variations. As the climate of a region is influenced by the region's geographic and physiographic features, it is therefore imperative to have an overview of the physiography of mainland India for undertaking a meaningful analysis of the temperature projections by exploring the influence of the physiography on the temperature of the future, if any. Figure 1(c) shows five major physiographic divisions into which mainland India can be broadly divided. These physiographic divisions together with distinct climatic features, manifested, inter alia, in localized heating, and hence temperature, cause the major weather systems of India to occur and move across the country. These weather systems are the southwest monsoon during June to September, the northeast monsoon during October to December, tropical cyclones during pre- and post-monsoon months, monsoon troughs or heat lows during summer, the western disturbances during winter, and local connective systems. Amongst these systems, the southwest monsoon is by far the most important one functioning as a major climatic moderator regulating India's temperature, bringing about 80% of the annual rainfall over India, and heavily influencing water availability, agricultural production, hydro-electric power generation, food grain price, and hence economy, of India. Noting the role and relevance of Southwest monsoon as a climate moderator in the study of future temperatures of India, the progress of Southwest monsoon given by the dates of its normal onset across the Indian territory from the end of May to the beginning of July is presented in Figure 1(d).

In order to examine the future temperature projections for meeting the objective of this study, 4,964 grid points at 0.25° × 0.25° resolution covering mainland India was considered. The selection of this resolution was based on the finest available resolution at which historical reference data over the whole of India were available and made use of in finalizing the modelling framework.

2.2 Datasets

In order to study the future temperature projections, outputs from 17 GCMs under CMIP6 were used. These 17 GCMs were selected based on the availability of the monthly outputs for the three temperature variables T_{max}, T_{mean} and T_{min} for SSP1-2.6, SSP2-4.5, SSP3-7.0 and SSP5-8.5 for the GCM projected period 2025-2100. A list of these GCMs is provided in Annexure Table A-1.

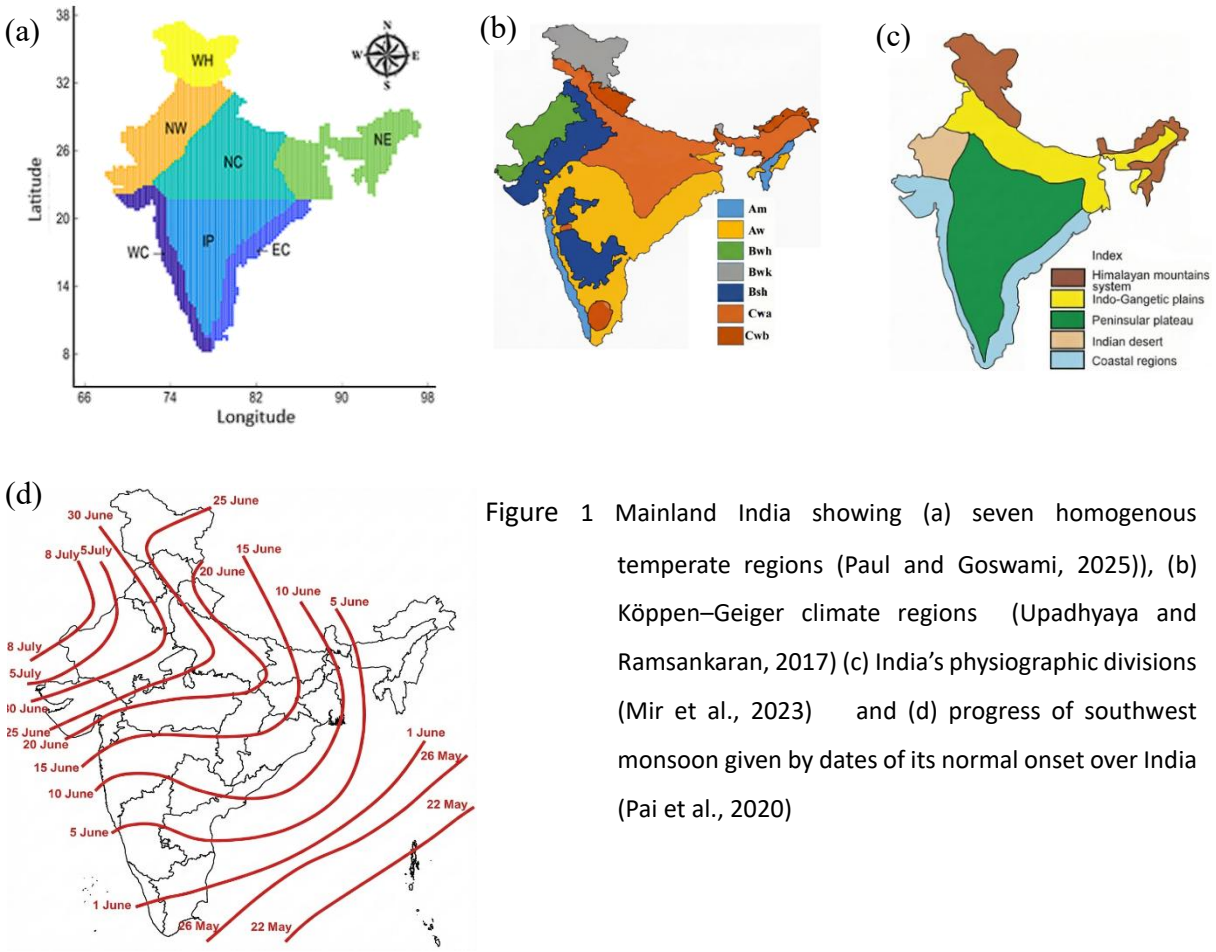


Figure 1 Mainland India showing (a) seven homogenous temperate regions (Paul and Goswami, 2025)), (b) Köppen–Geiger climate regions (Upadhyaya and Ramsankaran, 2017) (c) India's physiographic divisions (Mir et al., 2023) and (d) progress of southwest monsoon given by dates of its normal onset over India (Pai et al., 2020)

In order to compare the statistics of the future values with those of the historical values, reference data of the three temperature variables were taken from the European Centre for Medium Range Weather Forecasting (ECMWF)'s fifth-generation reanalysis product (ERA5) for the period from 1965 to 2014. The selection of the ERA5-sourced data for historical reference values of the temperature variables was made by these data performed well in several earlier temperature related studies (Lin et al., 2025; Pang et al., 2025).

3. Methodology

3.1 Examining future temperature projections

For analysing the future temperature projection, bias which is the systematic discrepancy between a model's output and the reference historical data (Teutschbein and Seibert, 2013), has to be corrected. Therefore, the selected 17 GCMs of CMIP6 are bias corrected using the methodology of Wavelet-integrated Adaptive Neuro Fuzzy Inference System (WANFIS), details of the methodlogy has been thorughly discussed in Paul and Goswami (2025). To improve the

reliability of climate projections, multi model ensemble (MMEs) technique is adopted which, combines selected GCMs using a performance-based weighting system. These weights reflect how accurately each component model reproduces historical trends, accounting for structural differences in physics and assumptions (Sanderson et al., 2015a). Consequently, by consolidating diverse model outputs, MMEs minimize inherite model uncertainites and the impact of outliers. Therefore, selected models are combined to form a multi model ensemble (MME) using the Granger-Ramanathan averaging (GRA) (Granger and Ramanathan, 1984) technique, details of the methodology has been thoroughly discussed in Nand et al., (2025). Using the bias corrected CMIP6 MME dataset, the annual and monthly values of the three selected temperature variables, T_{max}, T_{mean} and T_{min}, is generated over the future period from the year 2025 to 2100 by considering each of the four selected SSPs, namely SSP1-2.6, SSP2-4.5, SSP3-7.0 and SSP5-8.5. These values were produced for each of the 4,964 grid points at 0.25° × 0.25° resolution across mainland India. The generated future values of the temperature variables were then used to estimate the spatially-averaged as well as spatially distribtued grid-point-based values that are likely to occur in the future in the annual and monthly temporal resolutions under different SSPs.From the future values of temperature variables under different SSPs, the year-on-year annual average temperatures up to the year 2100 were estimated. By observing considerable variations of annual average temperatures from the current level and those in the past under different SSPs, the Year-on-year deviations of the monthly values of the future temperature variables from the corresponding values of the long-period means were studied, and the spatially aggregated extents of these deviations in four different ranges under different SSPs were explored. For this purpose, the month-wise values of the Long Period Averages (LPAs) were considered as being the Mean Reference Temperatures (MRTs) that were estimated from the BC-EN-corrected reference data over the long 50-year historical period 1965-2014, and the four MRT-based Groups (Gs) were adopted as below:

G1: < MRT –1.5°C, G2: MRT –1.5°C to MRT, G3: MRT to MRT +1.5°C, and G4: > MRT +1.5°C.

The month-wise MRTs and the month-wise deviations from the respective MRTs in respect of the temperature variables would allow for a structured evaluation of the warming magnitudes from both temporal as well as spatial considerations. Having noted the likely occurrence of trends from the temporal variations of the month-wise deviations of the temperature

variables of the future from the respective MRTs, the likely spatial distributions of the positive, negative or no trends of the month-wise average values of the three temperature variables for different SSPs over mainland India were studied, and the pattern of the spatially aggregated coverages of these month-wise trends were examined. Noting that the year-on-year annually averaged values of the future temperature variables differ considerably under different SSPs from their respective historical values, and also noting the likely occurrence of considerable variations of the monthly average values of the future temperature variables in varying spatially-aggregated extents across mainland India, the grid-point-based spatial distributions of the deviations of the annually averaged normal values of the future temperature variables from the LPAs under different SSPs were next analysed. Here, the term normal is used by considering its definition as given by the World Meteorological Organization (WMO, 2017)[1] that refers it 'to the most-recent 30-year period finishing in a year ending with 0'. Accordingly, two non-overlapping periods of 30 years for calculation of normals were considered in this study by designating the period 2071-2100 as far-future and the period 2041-2070 as near-future. The outcome of this analysis was the identification of the regions or parts of mainland land that are likely to be more vulnerable to future climate change impacts than the others.

Lastly, the Spatial distributions of trends of the annually averaged normal values of the future temperature variables were evaluated for different SSPs, and efforts were made to relate the characteristics of the likely trends in different parts of mainland India to the physiographic and climatological features of the respective areas.

3.2 Trend Analysis

For trend analyses, the Modified Mann–Kendall (MMK) test in particular and the Sen's Slope estimator were employed in this study by noting that trend detection in long-term temperature time series is likely to be influenced by serial correlation and non-normal data distribution (Yue et al., 2002). Monthly annual Trends were explored in order to evaluate the significance and magnitude of the future temperature trends across mainland India under different SSP scenarios by considering 4,964 grid points at 0.25° × 0.25° resolution.

[1] WMO Guidelines on the Calculation of Climate Normals, WMO No. 1203, 2017 Edition, pp. World Meteorological Organization (WMO), Geneva, Switzerland. ISBN: 978-92-63-11203-3.

Modified Mann- Kendall Test

The Mann–Kendall (MK) test (Mann, 1945) is a widely used non-parametric method for identifying monotonic trends in climatological and hydrological time series. However, the original MK test assumes that observations are independent. Since climate datasets often exhibit autocorrelation, this assumption can lead to inflated significance levels and overestimation of trend strength. To address this, the Modified Mann–Kendall (MMK) test proposed by (Hamed and Ramachandra Rao, 1998) was applied, which corrects the variance of the MK statistic to account for serial correlation. Detailed procedure of the method can be found in (Hamed and Ramachandra Rao, 1998).

Sen's Slope Estimator

The Sen's Slope estimator (Sen, 1968) is a non-parametric method used to quantify the magnitude of a monotonic trend. It calculates the median of all possible pairwise slopes between data points, providing a robust estimate that is resistant to outliers and non-normal data distribution. Detailed procedure of the method can be found in (Sen, 1968).

4. Results and Discussions

4.1 Year-on-year variations of annual average values of temperature variables from the past to the future

The chronological series of the average annual values of the three temperature variables T_{max}, T_{mean} and T_{min} for the historical period 1965-2014 and also for the GCM projected period 2025–2100 under four selected SSPs produced by employing the BC-EN approach by spatially averaging the values over all 4,964 grid points of mainland India at 0.25° × 0.25° resolution are plotted in Figure 2. From this figure it may be seen that, during the historical period 1965-2014, all three temperature variables experienced considerable year-on-year fluctuations with generally increasing trends. Similar observations were also made by (Kothawale and Rupa Kumar, 2005). During the future period 2025-2100, the year-on-year fluctuations are expected to be relatively small in comparison with those in the historical period. However, a distinct and persistent increasing trend of annual average values of all three temperature variables would occur until about the middle of this century across mainland India. The trends would be particularly pronounced along the three relatively higher emission pathways, namely SSP2-

4.5, SSP3-7.0 and SSP5-8.5, with the strength of the trends increasing with the increase of GHG concentrations. For the low-emisson scenario of the SSP1-2.6, the increasing trends of the annual average values would remain sustained until around the middle of this century before generally levelling during the second half of the century. Similar trends were also observed by (Norgate et al., 2024). For the low-emisson scenario of the SSP1-2.6, the increasing trends of the temperature variables are found to remain sustained until around the middle of this century before generally levelling during the second half of the century. In terms of the rates of increase of temperature, T_{min} is notably found to exhibit a generally faster rate of increase compared to T_{max}, implying a potential narrowing of the Monthly Temperature Range (MTR).

Another important inference that can be drawn from Figure 2 is that the divergence of each temperature variable in the second half of the century from the values during the histoical period and also from those until about the middle of the century, would be considerably high, particularly along the three relatively higher emission pathways, namely SSP2-4.5, SSP3-7.0 and SSP5-8.5. This signifies that the future temperature trajectories would be highly dependent on GHG concentrations and emission control strategies.

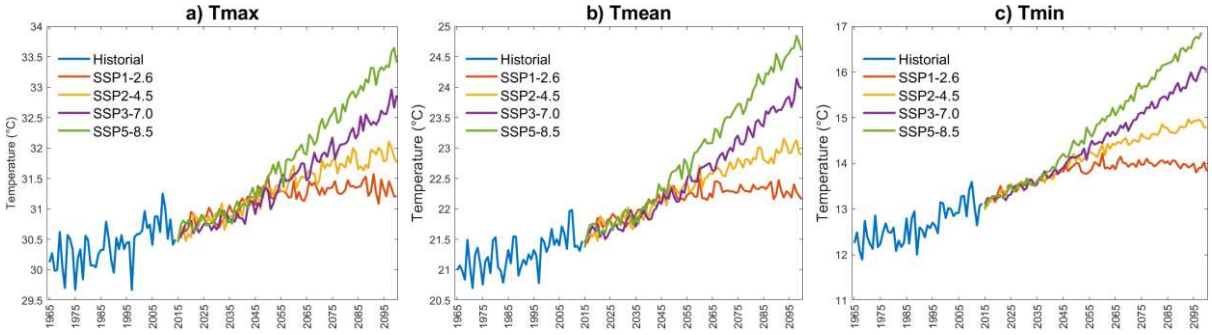


Figure 2 Annual average values of a) T_{max} b) T_{mean} and c) T_{min} of the historical period 1965-2014 and also for the GCM-projected period 2025-2100 for the selected SSPs

4.2 Variations of normal annual average temperatures in the near- and far-future relative to the current normals

In order to provide an overview of the future, the expected annual average values of the temperature variables T_{max}, T_{mean} and T_{min} that would be reckoned as being the normals during the near- and far-future periods of 2041-2070 and 2071-2100 respectively during the second half of this century are provided in Table 1. For comparative assessments, the current normal

for the historical period of 1991-2020 and also the expected annual average values of the temperature variables in the year 2100 under different emission scenarios are provided in this table. From this table, it may be found for the low-emission scenario SSP1-2.6 that, although the values of all three temperature variables T_{max}, T_{mean} and T_{min} in this scenario would increase from the corresponding current normal values, the increases from these normals to the corresponding values in the near- and far-future and to the annual values in the year 2100 are nearly equal.

Table 1 Normal average values of temperature (°C) in the near-future (1941-1970) and far-future (1971-2100) periods vis-à-vis the corresponding current normal over the period 1991-2020, and the values in the year 2100 with the corresponding % increases (in parenthesis)

Particulars	T_{max}			T_{mean}			T_{min}		
Historical period (1991-2020)	30.7			21.5			13.1		
Scenario for future projections	Near Future 1941-1970	Far Future 1971-2100	Year 2100	Near Future 1941-1970	Far Future 1971-2100	Year 2100	Near Future 1941-1970	Far Future 1971-2100	Year 2100
SSP 1-2.6	31.3 (1.8%)	31.3 (2.0%)	31.2 (1.6%)	22.2 (3.4%)	22.3 (3.7%)	22.2 (3.3%)	13.9 (6.6%)	14.0 (7.0%)	13.8 (5.7%)
SSP2-4.5	31.4 (2.1%)	31.8 (3.6%)	31.8 (3.5%)	22.4 (4.0%)	22.9 (6.3%)	22.9 (6.5%)	14.2 (8.6%)	14.7 (12.7%)	14.8 (13.4%)
SSP3-7.0	31.4 (2.2%)	32.3 (5.2%)	32.9 (7.1%)	22.4 (4.3%)	23.5 (9.2%)	24.0 (11.6%)	14.3 (9.8%)	15.5 (18.8%)	16.0 (22.6%)
SSP5-8.5	31.7 (3.1%)	33.0 (7.3%)	33.4 (8.8%)	22.8 (5.9%)	24.1 (12.2%)	24.6 (14.4%)	14.7 (12.4%)	16.2 (24.0%)	16.8 (28.7%)

The results presented in Figure 2 and Table 1 indicate the prospect of achieving stabilized climatic conditions in respect of temperature without major deviations from the conditions in the current normal period 1991-2020 in the case of low-emission scenario if created by strong global cooperations, lower consumptions, net-zero CO_2 emissions and effective mitigation measures towards achieving sustainable development. However, as expected, the normal annual averages of the three temperature variables are likely to consistently and considerably increase from their current normals to the corresponding values in the next-two non-overlapping 30-year periods of the future and also in the year 2100 with increasing severity of GHG concentrations. The severity of the increases from the current normal of 30.7°C, 21.5°C and 13.1°C of T_{max}, T_{mean} and T_{min} respectively can be particularly gauged from the future values in the year 2100 along SSP5-8.5 that show up as being 33.4°C, 24.6°C and 16.8°C, thereby working out to increases of 2.7°C i.e. 8.8%, 3.1°C i.e. 14.4% and 3.8°C i.e. 28.7%, corresponding to T_{max}, T_{mean} and T_{min} respectively. Overall, the future temperature

projections emphasize a robust warming signal across mainland India, with the magnitudes of change intensifying under higher emission pathways, underscoring the urgency of adopting strong climate mitigation measures to limit future temperature extremes. Further, these projections are generally consistent with the warming values for India as given in a report on Country-level warming projections by Berkley Earth[2], an independent non-profit organization having the objective of 'informing the global discourse on climate change', that states that India already attained '+1.0°C in 2022' vis-à-vis the corresponding value of +1.3°C for the world, and 'heading for around +3.4°C in 2100', these values being measured against the pre-industrial levels over the 1850–1900 period.

4.3 Year-on-year spatially aggregated deviations of the monthly values of the future temperature variables from the LPAs

The year-on-year deviations of monthly values of each of the three temperature variables T_{max}, T_{mean} and T_{min}, categorized into appropriate MRT-based groups amongst G1, G2, G3 and G4 over the future period 2025-2100 are presented in Figure 3, 4 and 5 respectively, with the respective MRTs being estimated from the long 50-year period 1965-2014. The four subplots in each of these figures correspond to the four selected SSPs, and exhibit the month-wise evolutions of the spatial coverage of future temperatures. The ordinate in each of these plots is divided into 12 blocks with each block representing one of the 12 months from January to December indicated by the three initial letters of each month, and the abscissa contains the years from 2025 to 2100. Each of these 12 blocks in each plot is kept equal in length representing the total number of grid-points, i.e. 4,964 at 0.25° × 0.25° resolution, and is stacked by four colour-coded parts representing four MRT-based groups.

It may be seen from Figure 3, 4 and 5 that, along SSP1–2.6, the temperature anomalies for T_{max} predominantly remain within G2–G3 throughout the remaining years of this century indicating limited warming within ±1.5°C of the historical long-period mean. Particularly, the aggregated spatial extents of T_{max} along SSP1-2.6 show relatively mild thermal conditions in most parts of mainland India during the pre-monsoon (March-May) and monsoon (June-September) seasons, and progressively increasing coverages year-on-year by temperatures exceeding the MRT+1.5°C threshold in the post-monsoon (October-December) and winter

[2] https://berkeleyearth.org/policy-insights/#content

(January–February) seasons with the maximum coverage by G4 occurring in the month of January.

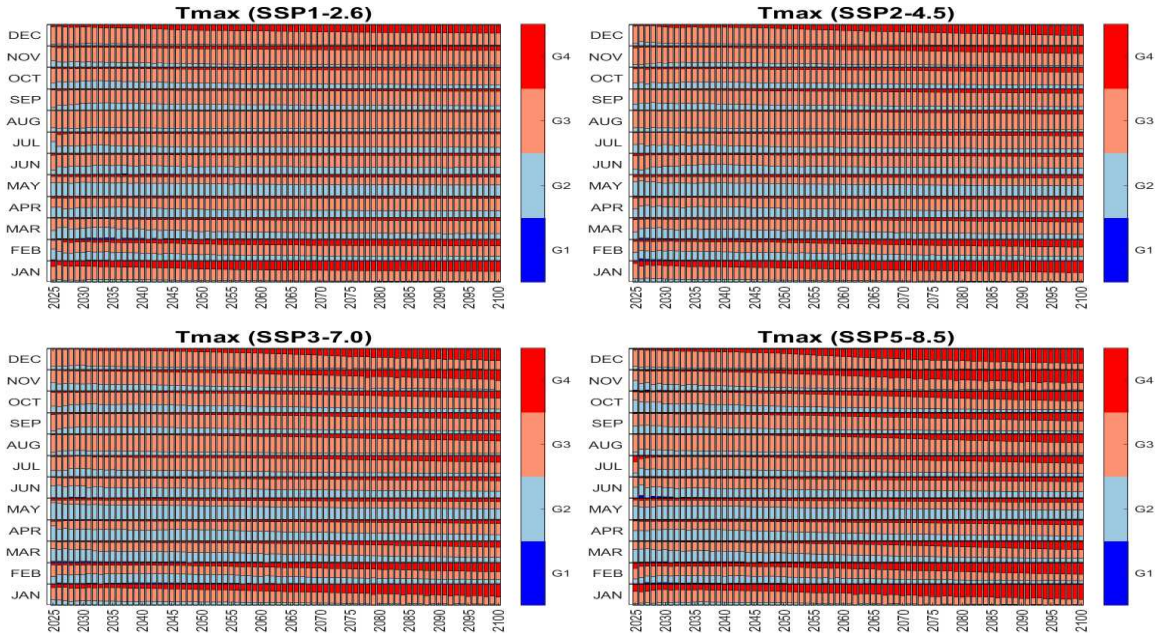


Figure 3 Year-on-year spatially aggregated extents of month-wise shares of G1, G2, G3 and G4 deviations of average values of T_{max} for different SSPs

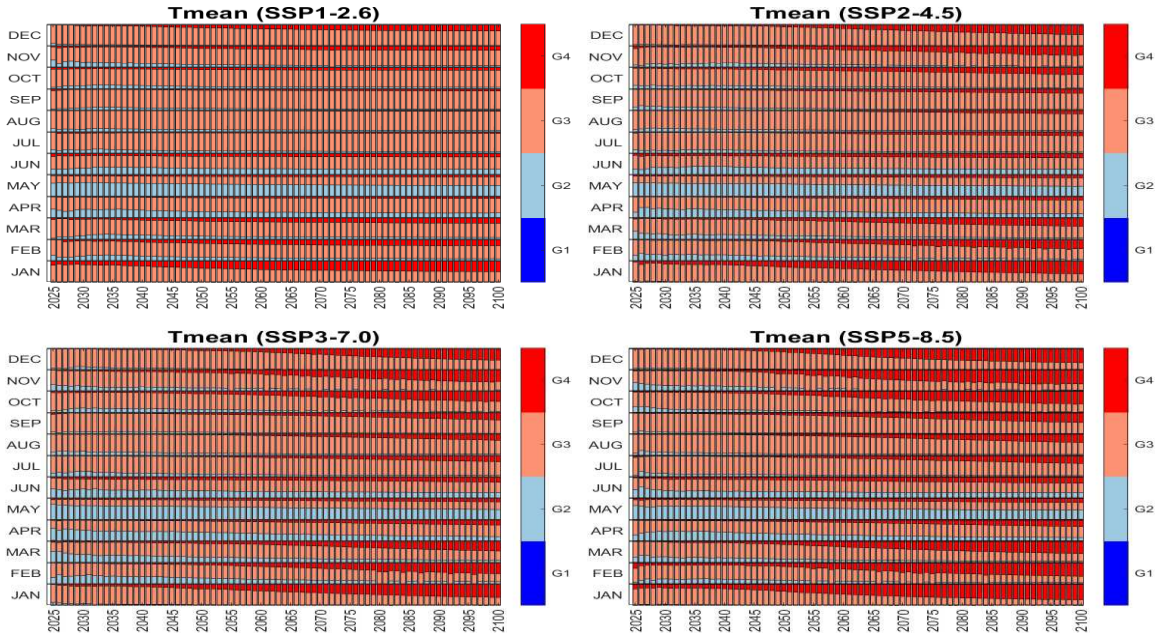


Figure 4 Year-on-year spatially aggregated extents of month-wise shares of G1, G2, G3 and G4 deviations of average values of T_{mean} for different SSPs

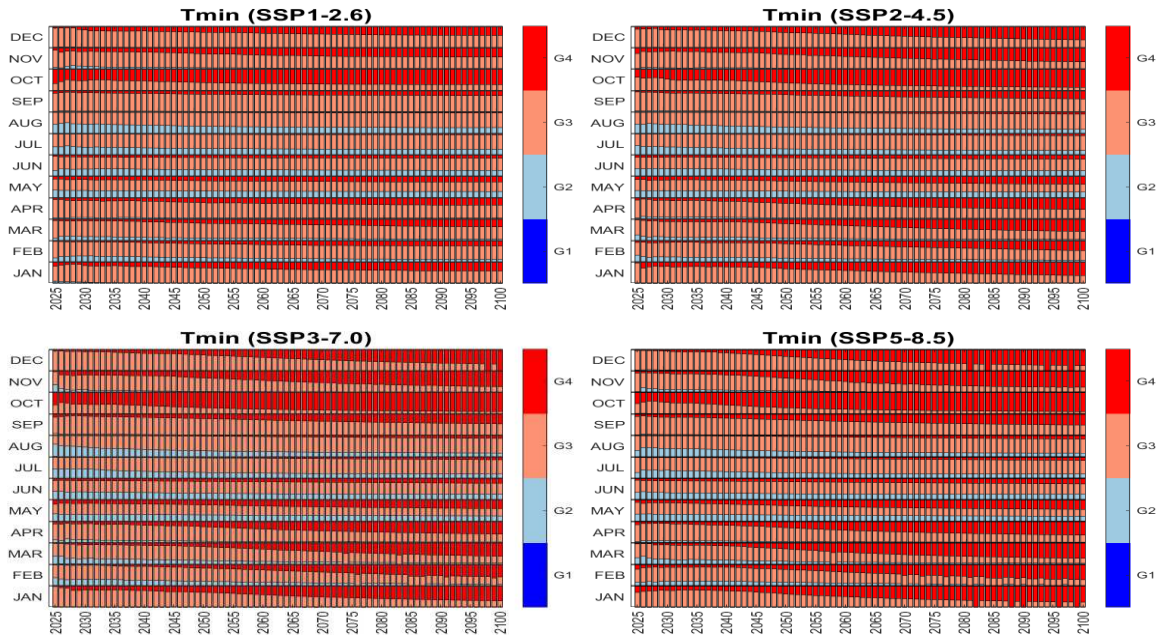


Figure 5 Year-on-year spatially aggregated extents of month-wise shares of G1, G2, G3 and G4 deviations of average values of T_{min} for different SSPs

The pattern of occurrence of the MRT-based groups in SSP1-2.6 is found to deviate for the T_{mean} and T_{min} variables from that for T_{max} with increasing shares of grid-points getting associated with G4 year-on-year with T_{min} displaying more aggravation in spatial coverage relative to T_{mean}. These patterns of occurrence of the MRT-based groups suggest the likelihood of increasing number of grid-points and hence spatial coverage of mainland India experiencing greater rises in nocturnal minimum temperatures than daytime maximum temperatures leading to the narrowing of MTR. Further, the general persistence of the G2 and G3 zones in respect of all three temperature variables in SSP1-2.6 during the pre-monsoon and monsoon seasons suggests that adoption of efficient emission reduction strategies in this pathway would help maintaining the near-stable climatic conditions with only minor deviations from the historical baseline during most part of the year whereas the increasing inclusions of the G4 zone in the stacks towards the winter and post-monsoon months suggest the need for relatively stringent mitigation measures capable of offsetting the increasing concentrations of GHGs due to seasonal cooling of the atmosphere during these months.

From the forecited figures, it may also be found that, with increasing severities of GHG concentrations, i.e. from SSP2-4.5 to SSP5-8.5 through SSP3-7.0, the patterns of deviations of monthly averages of all three temperature variables from the respective LPAs would shift gradually from the patterns along SSP1-2.6 towards increasing spatial coverages by monthly

average temperatures exceeding the G4 range, that would transition predominantly from the milder G3 range. These patterns indicating notable intensifications of temperature extremes by gradual shifts from one range of deviations to the next higher ranges of monthly average temperatures suggest enhanced spatial coverage by warming, generally throughout the year with mild exceptions during the four monsoon months from June to September, year-on-year. The patterns also reflect both daytime and nighttime heat accumulations in increasing areas of mainland India that are expected to become particularly widespread towards the end of the century.

Whereas the persistent presence of G4 across all SSPs for all three temperature variables, and gradual increase of its spatial coverage year-on-year reflects strong effects of radiative forcing, the transitions of T_{min} into the G4 deviation condition compared to T_{max} earlier in the future highlights the intensification of nocturnal warming—a signature of increasing GHG concentration and atmospheric moisture feedback from early years of the remaining period of the 21st century. Further, the systematic expansions of the G4 deviation condition of all temperature variables with time, particularly across non monsoon months, in the future along all SSPs underscore accelerated warming trajectories and narrowing windows for thermal stability, in a major part of the year in the future.

4.4 Trends and trend-wise spatial aggregation of month-wise average values of the future temperature variables

The results of monthly trends of the selected temperature variables over mainland India over the future period from 2025 to 2100 are plotted in terms of grid-point frequency in Figure 6 for demonstrating the temporal evolution of warming across different SSPs. This figure shows the aggregated spatial extents of coverages of mainland India by positive, negative, and no trends for each month under different selected SSP scenarios for the three selected temperature variables wherein the months from January to December are indicated along abscissa with the first letters of each month, and the number of grid points amongst the 4,964 grid points at 0.25° × 0.25° resolution are presented along the ordinate.

This figure shows the occurrence of dominant positive temperature trends across all SSP scenarios in all months and across aggregated spatial extents indicated by the total number of grid points in each month, with minor exceptions in the case of T_{max} only in the months of

June and July for the SSP1-2.6, thereby highlighting a generally consistent warming pattern over mainland India. As expected, this dominance generally increases progressively from SSP1-2.6 to SSP5-8.5, reflecting the increasing influence of GHG concentrations and radiative forcing on India's surface temperature dynamics.

Under the low-emission scenario SSP1-2.6, the majority of grid points accounting for about 60–70% of the total exhibit positive trends for T_{max}, T_{mean} and T_{min} with a noticeable presence of grid points showing no significant trend, particularly during the monsoon months of June–September. This indicates that under sustainable emission conditions, seasonal moderation due to monsoon rainfall and cloud cover still exerts a stabilizing influence on surface temperature. Negative trends are almost negligible with a very small number of grid points associated with negative trends appearing in the month of June, suggesting that cooling episodes are highly localized and transient.

In the moderate emission scenario, namely SSP2-4.5, the proportion of positive trends increases substantially, covering approximately 80–85% of grid points in all months. The variables T_{max} and T_{mean} show stronger warming during the pre-monsoon months of March–May and post-monsoon months of October–December, apparently influenced by increased land heating and reduced moisture feedback. The variable T_{min} also displays widespread positive trends particularly from November to March, indicating stronger warming during the winter season. The decline in 'No trend' extent of grid points relative to those in SSP1-2.6 signifies an increasing coherence in warming across spatial and temporal scales with the increasing severity of GHG concentrations.

Under the relatively more severe scenario SSP3-7.0 representing limited mitigation of GHG concentrations, security concerns, regional competition, environmental degradation, etc., the warming is found to intensify further with more than 85% of grid points generally demonstrating positive trends for T_{max}, T_{mean} and T_{min} in all months and only a small fraction showing no trend. The variable T_{min} is particularly found to exhibit a slightly greater frequency of positive trends than T_{max} like the pattern in the earlier SSP2-4.5 highlighting enhanced nighttime warming across mainland India, a key indicator of GHG-driven radiative imbalance. Conspicuously, there is a relative increase of the number of grid points associated with a negative trend in each of the three temperature variables along SSP3-7.0 in comparison with

the relatively less severe SSP2-4.5 that exhibits the likelihood of some areas experiencing a lowering of temperature indicating the possibilities of reducing concentrations of GHGs caused by increasing regional inequalities within the vast expanse of mainland India.

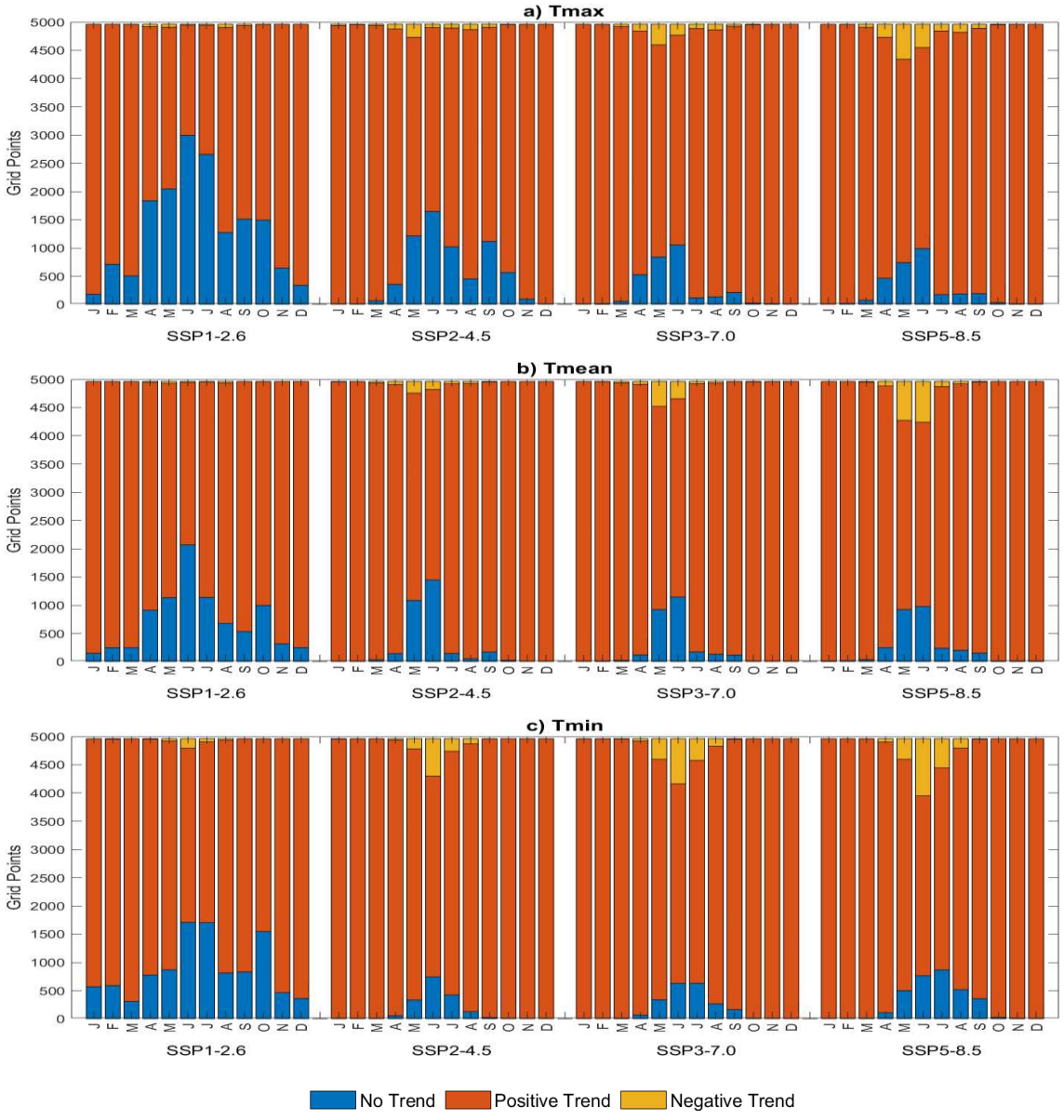


Figure 6 Aggregated spatial extents of month-wise Temperature Trends under four selected SSPs for a) T_{max} b) T_{mean} and c) T_{min}

The high-emission scenario, namely SSP5-8.5, reveals an almost uniform coverage of grid points associated with positive trends, accounting for more than 95% of all grid points, in all months thereby showing a generally consistent warming for T_{max}, T_{mean} and T_{min}. The spatial coverage of warming is most pronounced during the pre-monsoon and post-monsoon

seasons, suggesting stronger land–atmosphere coupling and reduced moisture buffering under elevated radiative forcing.

When comparing across variables, T_{min} generally exhibits the highest proportion of grid points with positive trends followed by T_{mean} and T_{max} along all four SSP pathways indicating a pattern of nonuniform warming across mainland India. This also indicates that nocturnal minimum temperatures are likely to rise faster in more areas than daytime maximum temperatures, leading to increasing narrowing of MTR, as was also concluded in the preceding subsection. Such a pattern would have significant implications on agriculture, energy demand, and human health as because reduced nighttime cooling would enhance heat stress and disrupt thermal comfort in more areas of the country. Seasonally, the non-monsoon months from October to May generally exhibit greater number of grid points with positive trend of all three temperature variables in all SSPs in comparison with those in the monsoon months of June–September, reflecting the damping effect of precipitation and cloud cover across mainland India during the monsoon season. Overall, the comparative analysis of the results presented in Figure 6 reveals a generally increasing spatial coverage of mainland India by warming from SSP1-2.6 to SSP5-8.5 that underscores India's increasing thermal vulnerability under high-emission trajectories. The difference in grid-point frequency between SSP5-8.5 and SSP1-2.6 also highlights the potential to mitigate significant warming through control of GHG concentrations. These findings collectively reaffirm the critical importance of adopting low-emission pathways to moderate temperature rise and sustain climatic stability across India.

4.5 Spatial Distributions of the deviations in annually averaged normal values of the far-future temperature variables from the LPAs

The spatial distributions of the deviations of the annual average temperature of the far future period 2071-2100 from the corresponding averages over the long historical period 1965-2014 are plotted in Figure 7. Here the period 2071-2100, would provide the normal values of the averages that would be expected in the far future under different SSPs. It may be found from this figure that the future deviations of all three temperature variables under the low-emission scenario of SSP1-2.6 would be mild and generally uniform across the whole of mainland India with minor exceptions in the case of T_{max} in particular in the hilly regions of the northwest India, that exhibit the possibility of larger increases in the maximum monthly temperatures in

the far future. Also, as expected, the magnitudes of the deviations of all three temperature variables are found to increase consistently from one SSP to the other with increasing severity of GHG concentrations.



Figure 7 Spatial distributions of deviations of the averages over far-future period 2071-2100 from the corresponding values of the historical LPAs during 1965-2014 for (a) to (d) T_{max} , (e) to (h) T_{mean} and (i) to (l) T_{min} under the four selected SSPs. Note: The colour scales at the bottom indicate variable-wise magnitudes of deviations

With reference to the Figure 1(a), it may be found from Figure 7 that, relatively large positive deviations of all temperature variables would occur consistently in the WH region and the hilly northern areas of the NE region along all SSPs with heightened values particularly under the pathways SSP2-4.5, SSP3-7.0 and SSP5-8.5 in comparison with the deviations across the rest of mainland India. Hence, these regions that are typically characterised by the high-altitude Himalayan Mountains system as shown in the physiographic map of India in Figure 1(c) would be relatively more vulnerable to high warming impacts along all future GHG emission scenarios. Prima facie, this inference regarding more intensified heating of the mountainous parts of the WH and NE regions in different SSPs would appear as being inconsistent with the patterns of relatively less intensifications across the rest of mainland India. However, the likely acceleration of warming of the Himalayan region in the future could be the results of the feedback from various atmospheric factors, namely snow-albedo, and black carbon and other aerosols as was found by Das and Meher (2019) and Ramachandran et al. (2023). Besides the impact of the feedback mechanisms, the data error due to coarse resolution of the raw GCM outputs for the mountainous regions could also be an influencing factor as also found by (Das et al., 2022) in inflating some of the results pertaining to remote and rugged terrains that are characteristic of the WH and the parts of the NE region. However, this latter aspect would call for more extensive studies, preferably with site-specific recorded data and GCM outputs of finer spatial resolution.

In contrast with the increased temperature amplifications in the WH and parts of the NE regions, the impacts of warming over the rest of India in terms of future deviations from the corresponding historical LPAs along SSP1-2.6 and SSP2-4.5 appear as being fairly uniform for all three temperature variables. However, as the severity of GHG concentrations increase, the impacts appear as being aggravated with increased spatial variations exhibited by larger deviations of all temperature variables in some parts than other. With reference to Figure 1(b), it may also be seen from Figure 7 that, along SSP3-7.0 and SSP5-8.5, all three temperature variables are expected to positively deviate considerably in varying degrees in the rest of India from the corresponding historical LPAs, with the NW region that is ‘arid, desert, hot (BWh)’ on its western side and ‘arid, steppe, hot (BSh)’ on its eastern side, and in parts of the NC region characterized by ‘temperate, dry winter, hot summer (Cwa)’ climate of the ‘Köppen-Geiger climate classification of India’ showing relatively large increases in comparison with the other

parts of the rest of India. The above observations reveal that the areas that are relatively dry are expected to be impacted more in terms of increased values of the temperature variables from the respective LPAs due to the absence of moderating influence of the humid atmosphere. In contrast, some parts of the coastal regions are expected to have relatively less deviations in respect of all three temperature variables along SSP3-7.0 and SSP5-8.5, possibly due to maritime influences as was also inferred in an earlier study by (Kantamaneni et al., 2022). Similar order of relatively low increase of temperature variables along SSP3-7.0 and SSP5-8.5 in some parts of the IP and NE regions are likely due to the influence of the tropical monsoon and vegetation cover. Overall, it was found from the spatially distributed future deviations of the average values from the corresponding historical LPAs of all three temperature variables that the varied amplifications across the Indian mainland could be likely due to the influence of the regionally diverse physiographic and climatic features of the expanse, and reflect the pervasive influence of intensified radiative forcing under unmitigated emission conditions. This observation aligns with the findings from other studies, such as those conducted over South Asia using CMIP5 models (Yang et al., 2020) and CMIP6 models (Salehie et al., 2022).

4.6 Spatial distributions of trends of the annually averaged values of the future temperature variables

The grid-point-wise spatial distributions of the trends of the annual average values of the three selected temperature variables per year along each of the four selected SSPs over mainland India over the remaining part of this century are presented in Figure 8. The trends in this figure are indicated by Sen's Slopes over the long future period from 2025 to 2100. The spatial distributions of the trends in this figure reveal that, in the case of the variable T_{max}, some parts of the southern sides of the Gangetic plains on the NC region, the valley areas of the NE region having a 'Temperate, dry winter, hot summer (Cwa)' climate, and the eastern parts of the IP region having a 'Tropical, monsoon (Am)' climate are not likely to experience significant trends along all SSPs, and that some parts on the west and northwest of India having an 'arid, steppe, hot' (Bsh) climate also show a similar pattern of trends of T_{max} under the SSP1-2.6 scenario.

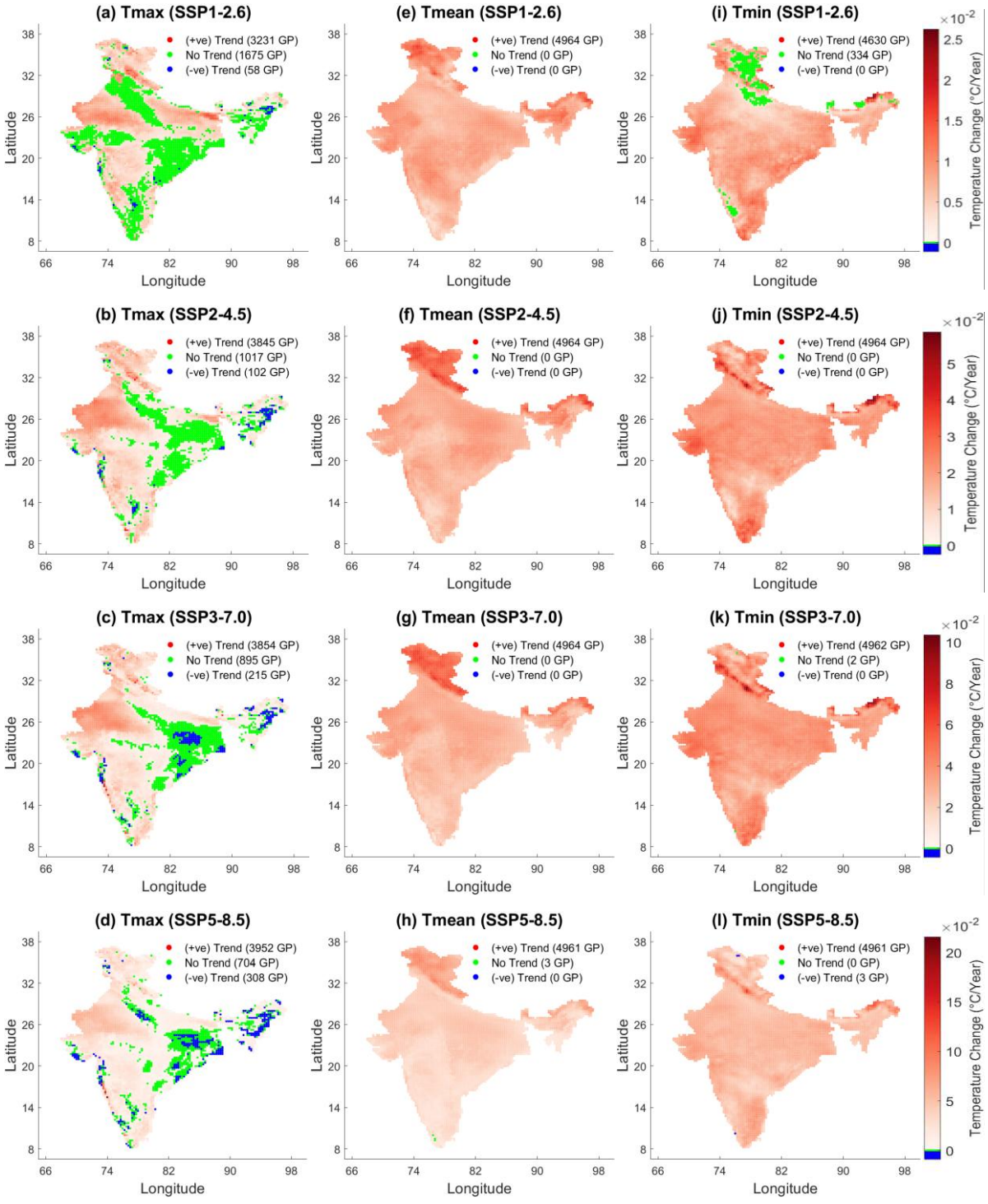


Figure 8 Spatial distributions of trends of (a) to (d) T_{max} , (e) to (h) T_{mean} and (i) to (l) T_{min} under the four selected SSPs. Note: The colour scales on the right indicate SSP-wise magnitudes of trends with reddish shades for varying degrees of positive trends (warming), green for near-neutral or statistically insignificant changes, and blue for negative trends (cooling).

It may also be found from the blue-coloured parts shown scattered in these plots that, for all SSPs, some areas on the northeast, east and west of India even show negative trends of T_{max}

521 with the number of grid-points having negative trends increasing with increasing severity of
522 GHG concentrations. These patterns of trends of T_{max} across SSPs are likely caused by the
523 moderating impacts of the major annual weather phenomenon of the southwest monsoon of
524 India, the Bay of Bengal component of which predominantly progresses from the eastern and
525 northeastern sides of the country towards the northwest, and the Arabian Sea component of
526 which moves from the southwest towards the north over a considerable period during
527 summer months as shown in Figure 1(d). Over the rest of India, the trends of T_{max} along
528 different SSPs are found as being positive with the hot and arid desert area occupied by the
529 Thar Desert in the state of Rajasthan in the NW region, as shown in the map of the
530 physiographic divisions of India in Figure 1(c), particularly showing relatively strong positive
531 trends of T_{max} in comparison with the positive trends of T_{max} in other parts of India. Whereas
532 the dearth of atmospheric moisture in the desert areas is likely to cause more intensification
533 of heat under scenarios of increased GHG concentrations, the availability of atmospheric
534 moisture, generally related to monsoon, before, during and after its occurrence over the rest
535 of the Indian mainland impart a moderating effect on T_{max}, thereby showing considerably
536 weaker trends of increase. The patterns of trends as exhibited in plots (e) to (h) and (i) to (l)
537 in Figure 8 for T_{mean} and T_{min} respectively generally remain similar across mainland India from
538 one SSP to another, and, as expected, exhibit increasing magnitudes of positive trends with
539 increasing severity of GHG concentrations with the exception in the case of T_{min} along SSP1-
540 2.6 that shows the existence of insignificant or no trend in some parts of India. With reference
541 to the Figure 1(a), (b) and (c) and from plots (e) to (h) in Figure 8, it may be found that, in the
542 case of T_{mean}, considerably large positive trends occur consistently along all SSPs in the WH
543 region and the hilly areas of the NE region implying that these regions would be relatively
544 more prone to high warming impacts along all SSP pathways. By contrast, some parts of the
545 coastal regions and some parts experiencing tropical climate in the IP region show relatively
546 moderate warming trends. In the case of the rest of India, relatively uniform trends of
547 amplification of the mean temperature T_{mean} across the expanse is found to occur under the
548 scenarios of higher emissions with the conditions along SSP5-8.5 particularly showing more
549 homogenized trends. This observation indicates that the annual mean monthly temperature
550 over the rest of India would increase at comparable rates across different physiographic and
551 climatic divisions of the expanse under the severe GHG concentration scenario, thereby
552 implying widespread impacts of the factors aggravating GHG concentrations.

In the case of T_{min}, the plots (i) to (l) in Figure 8 indicate that the minimum temperatures in forest-covered high mountainous parts of the WH, NE and WC regions are not likely to have significant trends under the low-emission scenario of SSP1-2.6 that, as stated earlier, is reflective of the impacts of strong global cooperations, lower consumptions, net-zero CO_2 emissions and effective mitigation measures towards achieving sustainable development. However, in these regions, the mitigating impacts of forests and relatively less anthropogenic actions associated with the SSP1-2.6 scenario seem to die out, and the emission-induced enhancements of the minimum temperature values seem to take over with increasing GHG concentrations, particularly in the Outer or Siwalik Himalayan parts of the WH region, parts of the hilly states of Sikkim and Arunachal Pradesh of the NE region that have 'polar, frost (EF)' type of climate, and the parts of the Western Ghat mountains in the WC region that have a 'tropical, rainforest (Af)' climate. Over the rest of the Indian mainland, the strengths of positive trends of T_{min} continue increasing with increasing GHG concentrations although the patterns of spatial variations of trends appear as being similar under different SSPs of higher emission scenarios.

Conspicuously, the positive trends of T_{max} over the whole of mainland India appear as being considerably weaker than those of T_{mean} and T_{min} particularly along SSP2-4.5, SSP3-7.0 and SSP5-8.5, and the positive trends of T_{mean} are found to be considerably weaker than those of T_{min}. These observations generally indicate pervasive nocturnal heat accumulations during nighttime, leading to reductions in MTR that was consistent with the with the inference drawn by (Vinnarasi et al., 2017).

5. Conclusions

Overall, it was found from the analysis of the future temperature projections that, generally, a distinct and persistent warming of annual average values of all three temperature variables would occur across mainland India along all SSPs in the future period 2025-2100, with the rate and magnitude of warming increasing with increasing severity of GHG concentrations. Importantly, the divergence of each temperature variable in the second half of the century from the values during the histoical period and also from those until about the middle of the century, would be considerably high, particularly along the three relatively higher emission pathways, namely SSP2-4.5, SSP3-7.0 and SSP5-8.5. In terms of the rates of increase of the

583 temperature variables, T_{min} is notably found to exhibit a generally faster rate of increase
584 compared to T_{max}, implying a potential narrowing of the MTR that would have significant
585 implications on agriculture, energy demand, and human health from reduced nighttime
586 cooling, enhanced heat stress and disruption of thermal comfort in extensive areas of the
587 country.

588 It also emerged from the study that distinct patterns of the future deviations of the normal
589 annual average values of the temperature variables from the corresponding current normals
590 as well as those of the trends of the temperature variables in the remaining part of this
591 century are discernible in distinct physiographically and climatologically different regions of
592 mainland India. These patterns are particularly conspicuous in the Western Himalayan region
593 and the hilly areas of the North-Eastern region exhibiting considerably more amplifications as
594 well as strong increasing trends of the temperature variables and hence considerably more
595 vulnerability to climate change relative to the rest of India. In essence, these regions bordering
596 the entire north-western, northern and the north-eastern parts of the country are occupied
597 by the Himalayan Mountain ranges characterized by high altitudes, perennial snow-clad peaks
598 and about 15,000 glaciers that provide perennial meltwater into the Indus, the Ganges and
599 the Brahmaputra Rivers, and collectively act as a lifeline of about 500 million people in the
600 Indian subcontinent[3]. Whereas the increase in the values of temperature variables in these
601 regions in the future along different SSPs associated with higher GHG concentrations could be
602 caused by the mechanisms of feedback from various atmospheric factors, namely snow-
603 albedo, and black carbon and other aerosols, etc., the impact of these increases causing
604 reduction of flows in three major rivers can be disastrous to the communities, economies and
605 infrastructures of mainland India. The distinct patterns of increases of the values and the
606 trends of temperature variables are also exhibited in the arid and hot regions of western India
607 that includes the Thar desert of India, and suffers from the risks of increasing desertification
608 of the region. The increases in the monthly and annual average values of the temperature
609 variables and the positive trends of these values over the rest of India with increasing GHG
610 concentrations, particularly along SSP2-4.5, SSP3-7.0 and SSP5-8.5, are expected to be
611 relatively milder than the north, the north-west and the northern parts of the north east India,
612 primarily due to the moderating effects of the monsoon rainfall. However, these increases and

[3] https://www.worldwateratlas.org/narratives/melting-glaciers/glaciermelt/#glaciers-melt-water-resource

613 the temporal and spatial alterations of these increases over the regions in the rest of India still
614 indicate the increasing risks of exposures to and hence increasing vulnerabilities of the
615 communities, economies and infrastructures almost all over the regions from the increasing
616 frequencies and amplifications of hydrometeorological extremes of heatwaves, agricultural
617 and hydrological droughts, pluvial and fluvial floods, tropical and extratropical cyclones, etc.
618 besides from shifts in the onset of normal monsoons, phrenological shifts, impacts on season-
619 dependent agricultural productions, increasing occurrences of forest fires, etc.

620 The projected strong and spatially extensive future warming and warming trends over
621 mainland India under increasing GHG concentrations highlight the urgent need for planning,
622 implementing and adopting adaptive measures and low-emission policies for the future with
623 the objective of mitigating the impacts of increasing temperature from GHG-induced climate
624 change, creating resilience against these impacts, minimizing the socio-environmental
625 consequences thereof.

626 **Author Contributions**

627 The first author conceptualized, analysed, and prepared graphical outputs of the research.
628 The second author suggested improvements on the methodology and presentation of results,
629 and prepared the manuscript.

630 **Conflict of Interest Statement**

631 The authors declare no conflict of interest.

632 **Competing Interests**

633 The authors have no relevant financial or non-financial interests to disclose.

634 **Funding**

635 This research received no funding from external sources.

636 **Data Availability Statement**

637 Raw simulated outputs of GCMs of the CMIP6 phase are available at https://esgf-
638 node.llnl.gov/projects/cmip6/

639 **Acknowledgement**

640 The authors are thankful to the anonymous reviewers for their valuable suggestions and
641 insightful comments.

642 **ORCID**

643 Avijit Paul: 0000-0001-9388-9571

Monomoy Goswami: 0000-0003-1380-6276

References

Atkinson, D., Porter, J.R., 1996. Temperature, plant development and crop yields. Trends in Plant Science 1, 119–124. https://doi.org/10.1016/S1360-1385(96)90006-0

Burgmer, T., Hillebrand, H., 2011. Temperature mean and variance alter phytoplankton biomass and biodiversity in a long-term microcosm experiment. Oikos 120, 922–933. https://doi.org/10.1111/j.1600-0706.2010.19301.x

Das, S., Giorgi, F., Coppola, E., Panicker, A.S., Gautam, A.S., Nair, V.S., Giuliani, G., 2022. Linkage between the absorbing aerosol-induced snow darkening effects over the Himalayas-Tibetan Plateau and the pre-monsoon climate over northern India. Theor Appl Climatol 147, 1033–1048. https://doi.org/10.1007/s00704-021-03871-y

Dash, S.K., Mamgain, A., 2011. Changes in the Frequency of Different Categories of Temperature Extremes in India. https://doi.org/10.1175/2011JAMC2687.1

Frederick, K.D., Major, D.C., 1997. Climate Change and Water Resources. Climatic Change 37, 7–23. https://doi.org/10.1023/A:1005336924908

Granger, C.W.J., Ramanathan, R., 1984. Improved methods of combining forecasts. Journal of Forecasting 3, 197–204. https://doi.org/10.1002/for.3980030207

Hamed, K.H., Ramachandra Rao, A., 1998. A modified Mann-Kendall trend test for autocorrelated data. Journal of Hydrology 204, 182–196. https://doi.org/10.1016/S0022-1694(97)00125-X

Huang, J., Tang, X., Jones, P., Hao, T., Tundokova, R., Walmsley, C., Lannon, S., Frost, P., Jackson, J., 2024. Mapping pedestrian heat stress in current and future heatwaves in Cardiff, Newport, and Wrexham in Wales, UK. Building and Environment 251, 111168. https://doi.org/10.1016/j.buildenv.2024.111168

Kantamaneni, K., Panneer, S., Krishnan, A., Shekhar, S., Bhat, L., R, A.K., Rice, L., 2022. Appraisal of climate change and cyclone trends in Indian coastal states: a systematic approach towards climate action. Arab J Geosci 15, 814. https://doi.org/10.1007/s12517-022-10076-8

Kothawale, D.R., Rupa Kumar, K., 2005. On the recent changes in surface temperature trends over India. Geophysical Research Letters 32. https://doi.org/10.1029/2005GL023528

Li, Z., Fang, G., Chen, Y., Duan, W., Mukanov, Y., 2020. Agricultural water demands in Central Asia under 1.5 °C and 2.0 °C global warming. Agricultural Water Management 231, 106020. https://doi.org/10.1016/j.agwat.2020.106020

Lin, J., Zhang, H., Wei, S., Xu, Q., Li, Z., Li, Q., 2025. Outstanding performance of ERA5 reanalysis temperature in China since the 1950s and quantification of its abnormal error in 1965–1966. Quarterly Journal of the Royal Meteorological Society n/a, e5042. https://doi.org/10.1002/qj.5042

Linacre, E.T., 1977. A simple formula for estimating evaporation rates in various climates, using temperature data alone. Agricultural Meteorology 18, 409–424. https://doi.org/10.1016/0002-1571(77)90007-3

Mann, H.B., 1945. Nonparametric Tests Against Trend. Econometrica 13, 245–259. https://doi.org/10.2307/1907187

Nand, V., Qi, Z., Ma, L., Helmers, M.J., Madramootoo, C.A., Smith, W.N., Zhang, T., Weber, T.K.D., Pattey, E., Li, Z., Wang, J., Jin, V.L., Jiang, Q., Tenuta, M., Trout, T.J., Cheng, H., Harmel, R.D., Kimball, B.A., Thorp, K.R., Boote, K.J., Stockle, C., Suyker, A.E., Evett, S.R.,

Brauer, D.K., Coyle, G.G., Copeland, K.S., Marek, G.W., Colaizzi, P.D., Acutis, M., Alimagham, S.M., Archontoulis, S., Babacar, F., Barcza, Z., Basso, B., Bertuzzi, P., Constantin, J., De Antoni Migliorati, M., Dumont, B., Durand, J.-L., Fodor, N., Gaiser, T., Garofalo, P., Gayler, S., Giglio, L., Grant, R., Guan, K., Hoogenboom, G., Kim, S.-H., Kisekka, I., Lizaso, J., Masia, S., Meng, H., Mereu, V., Mukhtar, A., Perego, A., Peng, B., Priesack, E., Shelia, V., Snyder, R., Soltani, A., Spano, D., Srivastava, A., Thomson, A., Timlin, D., Trabucco, A., Webber, H., Willaume, M., Williams, K., van der Laan, M., Ventrella, D., Viswanathan, M., Xu, X., Zhou, W., 2025. Evaluation of multimodel averaging approaches for ensembling evapotranspiration and yield simulations from maize models. Journal of Hydrology 661, 133631. https://doi.org/10.1016/j.jhydrol.2025.133631

Norgate, M., Tiwari, P.R., Das, S., Kumar, D., 2024. On the heat waves over India and their future projections under different SSP scenarios from CMIP6 models. International Journal of Climatology 44, 973–995. https://doi.org/10.1002/joc.8367

Pang, N., Kong, H., Wong, C., Li, Z., Du, Y., Leung, J.C.-H., 2025. A CNN-Based Downscaling Model for Macau Temperature Prediction Using ERA5 Reanalysis Data. Applied Sciences 15, 5321. https://doi.org/10.3390/app15105321

Paul, A., Goswami, M., 2025. An Adaptive Neuro-Fuzzy Inference System (ANFIS) and a Wavelet-Integrated ANFIS (WANFIS) for Univariate Bias-Correction of GCM -Simulated Temperature. Intl Journal of Climatology e8816. https://doi.org/10.1002/joc.8816

Peng, X., Yu, M., Chen, H., Zhou, B., Shi, Y., Yu, L., 2023. Projections of wildfire risk and activities under 1.5 °C and 2.0 °C global warming scenarios. Environ. Res. Commun. 5, 031002. https://doi.org/10.1088/2515-7620/acbf13

Perkins-Kirkpatrick, S.E., Gibson, P.B., 2017. Changes in regional heatwave characteristics as a function of increasing global temperature. Sci Rep 7, 12256. https://doi.org/10.1038/s41598-017-12520-2

Revadekar, J.V., Kothawale, D.R., Patwardhan, S.K., Pant, G.B., Rupa Kumar, K., 2012. About the observed and future changes in temperature extremes over India. Nat Hazards 60, 1133–1155. https://doi.org/10.1007/s11069-011-9895-4

Riahi, K., van Vuuren, D.P., Kriegler, E., Edmonds, J., O'Neill, B.C., Fujimori, S., Bauer, N., Calvin, K., Dellink, R., Fricko, O., Lutz, W., Popp, A., Cuaresma, J.C., Kc, S., Leimbach, M., Jiang, L., Kram, T., Rao, S., Emmerling, J., Ebi, K., Hasegawa, T., Havlik, P., Humpenöder, F., Da Silva, L.A., Smith, S., Stehfest, E., Bosetti, V., Eom, J., Gernaat, D., Masui, T., Rogelj, J., Strefler, J., Drouet, L., Krey, V., Luderer, G., Harmsen, M., Takahashi, K., Baumstark, L., Doelman, J.C., Kainuma, M., Klimont, Z., Marangoni, G., Lotze-Campen, H., Obersteiner, M., Tabeau, A., Tavoni, M., 2017. The Shared Socioeconomic Pathways and their energy, land use, and greenhouse gas emissions implications: An overview. Global Environmental Change 42, 153–168. https://doi.org/10.1016/j.gloenvcha.2016.05.009

Sakai, A., Larcher, W., 1987. Low Temperature and Frost as Environmental Factors, in: Sakai, A., Larcher, W. (Eds.), Frost Survival of Plants: Responses and Adaptation to Freezing Stress. Springer, Berlin, Heidelberg, pp. 1–20. https://doi.org/10.1007/978-3-642-71745-1_1

Salehie, O., Ismail, T. bin, Hamed, M.M., Shahid, S., Idlan Muhammad, M.K., 2022. Projection of Hot and Cold Extremes in the Amu River Basin of Central Asia using GCMs CMIP6. Stoch Environ Res Risk Assess 36, 3395–3416. https://doi.org/10.1007/s00477-022-02201-6

Sen, P.K., 1968. Estimates of the Regression Coefficient Based on Kendall's Tau. Journal of the American Statistical Association 63, 1379–1389. https://doi.org/10.1080/01621459.1968.10480934

Shen, X., Liu, B., 2016. Changes in the timing, length and heating degree days of the heating season in central heating zone of China. Sci Rep 6, 33384. https://doi.org/10.1038/srep33384

Stillman, J.H., 2019. Heat Waves, the New Normal: Summertime Temperature Extremes Will Impact Animals, Ecosystems, and Human Communities. Physiology 34, 86–100. https://doi.org/10.1152/physiol.00040.2018

Sutherst, R.W., Constable, F., Finlay, K.J., Harrington, R., Luck, J., Zalucki, M.P., 2011. Adapting to crop pest and pathogen risks under a changing climate. WIREs Climate Change 2, 220–237. https://doi.org/10.1002/wcc.102

Thornton, P., Nelson, G., Mayberry, D., Herrero, M., 2021. Increases in extreme heat stress in domesticated livestock species during the twenty-first century. Global Change Biology 27, 5762–5772. https://doi.org/10.1111/gcb.15825

Upadhyaya, S., Ramsankaran, R., 2017. Comprehensive inter-comparison of INSAT multispectral rainfall algorithm estimates and TMPA 3B42-RT V7 estimates across different climate regions of India during southwest monsoon period. Environ Monit Assess 190, 45. https://doi.org/10.1007/s10661-017-6411-7

Vinnarasi, R., Dhanya, C.T., Chakravorty, A., AghaKouchak, A., 2017. Unravelling Diurnal Asymmetry of Surface Temperature in Different Climate Zones. Sci Rep 7, 7350. https://doi.org/10.1038/s41598-017-07627-5

Wan, K.K.W., Li, D.H.W., Liu, D., Lam, J.C., 2011. Future trends of building heating and cooling loads and energy consumption in different climates. Building and Environment 46, 223–234. https://doi.org/10.1016/j.buildenv.2010.07.016

Yang, Y., Jin, C., Ali, S., 2020. Projection of heat wave in China under global warming targets of 1.5 °C and 2 °C by the ISIMIP models. Atmospheric Research 244, 105057. https://doi.org/10.1016/j.atmosres.2020.105057

Yue, S., Pilon, P., Cavadias, G., 2002. Power of the Mann–Kendall and Spearman's rho tests for detecting monotonic trends in hydrological series. Journal of Hydrology 259, 254–271. https://doi.org/10.1016/S0022-1694(01)00594-7

ANEXURES

Annexure A-1 Details of the GCMs of CMIP6 considered in this study

Sl. No.	Model name	Resolution (Long × Lat)	Institution
1	ACCESS-CM2	192×144	Commonwealth Scientific and Industrial Research Organisation and Australian Research Council Centre of Excellence for Climate System Science, Australia
2	ACCESS-ESM1-5	192×145	
3	AWI-CM-1-1-MR	384x192	Alfred Wegener Institute, Helmholtz Centre for Polar and Marine Research, Bremerhaven, Germany
4	CMCC-ESM2	288x192	Fondazione Centro Euro-Mediterraneo sui Cambiamenti Climatici, Italy

Sl. No.	Model name	Resolution (Long × Lat)	Institution
5	CAS-ESM2-0	362 x 196	Chinese Academy of Sciences Earth System Model version 2.0
6	EC-Earth3-Veg	512×256	EC-Earth-Consortium
7	EC-Earth3-Veg-LR	320x160	
8	EC-Earth3	512×256	
9	FGOALS-g3	180×80	Chines Academy of Sciences, China
10	GFDL-ESM4	288×180	Geophysical Fluid Dynamics Laboratory, USA
11	INM-CM4-8	180×120	Institute for Numerical Mathematics, Russia
12	INM-CM5-0	180×120	
13	IPSL-CM6A-LR	144×143	Institut Pierre-Simon Laplace, France
14	MIROC6	256×128	JAMSTEC, AORI, NIES, R-CCS, Japan
15	MPI-ESM1-2-HR	384×192	Max Planck Institute for Meteorology, Germany
16	MPI-ESM1-2-LR	192×96	
17	MRI-ESM2-0	320×160	Meteorological Research Institute, Japan

769